Resolution enhancement for low-temperature scanning microscopy by cryo-immersion

Michael Metzger,[1] Alexander Konrad,[1] Sepideh Skandary,[1] Imran Ashraf,[1] Alfred J. Meixner[1] and Marc Brecht[1,2,3,*]

[1] *Institute of Physical and Theoretical Chemistry, University of Tuebingen, Tuebingen, Germany*

[2] *Zurich University of Applied Science, Institute of Applied Mathematics and Physics, Winterthur, Switzerland*

[3] *Process Analysis and Technology (PA&T), Reutlingen Research Institute, Reutlingen University, Reutlingen, Germany*

[*] *marc.brecht@uni-tuebingen.de*

Abstract: Here we report a simple way to enhance the resolution of a confocal scanning microscope under cryogenic conditions. Using a microscope objective (MO) with high numerical aperture ($NA = 1.25$) and 1-propanol as an immersion fluid with low freezing temperature we were able to reach an imaging resolution at 160 K comparable to ambient conditions. The MO and the sample were both placed inside the inner chamber of the cryostat to reduce distortions induced by temperature gradients. The image quality of our commercially available MO was further enhanced by scanning the sample (sample scanning) in contrast to beam scanning. The ease of the whole procedure marks an essential step towards the development of cryo high-resolution microscopy and correlative light and electron cryo microscopy (cryoCLEM).

OCIS codes: (180.1790) Confocal microscopy; (180.2520) Fluorescence microscopy; (180.5810) Scanning microscopy; (110.0180) Microscopy; (330.6130) Spatial resolution.

References and links

1. M. Minsky, "Memoir on inventing the confocal scanning microscope," Scanning **10**(4), 128–138 (1988).
2. G. Lin, M. K. Chawla, K. Olson, C. A. Barnes, J. F. Guzowski, C. Bjornsson, W. Shain, and B. Roysam, "A multi-model approach to simultaneous segmentation and classification of heterogeneous populations of cell nuclei in 3D confocal microscope images," Cytometry A **71A**(9), 724–736 (2007).
3. A. Drechsler, M. A. Lieb, C. Debus, A. J. Meixner, and G. Tarrach, "Confocal microscopy with a high numerical aperture parabolic mirror," Opt. Express **9**(12), 637–644 (2001).
4. E. Abbe, "Beitraege zur Theorie des Mikroskops und der mikroskopischen Wahrnehmung," Arch. Mikrosk. Anat. **9**(1), 413–418 (1873).
5. M. Bates, B. Huang, G. T. Dempsey, and X. W. Zhuang, "Multicolor super-resolution imaging with photo-switchable fluorescent probes," Science **317**(5845), 1749–1753 (2007).
6. E. Betzig, G. H. Patterson, R. Sougrat, O. W. Lindwasser, S. Olenych, J. S. Bonifacino, M. W. Davidson, J. Lippincott-Schwartz, and H. F. Hess, "Imaging intracellular fluorescent proteins at nanometer resolution," Science **313**(5793), 1642–1645 (2006).
7. M. Friedenberger, M. Bode, A. Krusche, and W. Schubert, "Fluorescence detection of protein clusters in individual cells and tissue sections by using toponome imaging system: sample preparation and measuring procedures," Nat. Protoc. **2**(9), 2285–2294 (2007).

#261789 Received 18 Apr 2016; revised 27 May 2016; accepted 27 May 2016; published 6 Jun 2016

8. S. W. Hell, M. Dyba, and S. Jakobs, "Concepts for nanoscale resolution in fluorescence microscopy," Curr. Opin. Neurobiol. **14**(5), 599–609 (2004).
9. S. Manley, J. M. Gillette, G. H. Patterson, H. Shroff, H. F. Hess, E. Betzig, and J. Lippincott-Schwartz, "High-density mapping of single-molecule trajectories with photoactivated localization microscopy," Nat. Methods **5**(2), 155–157 (2008).
10. M. J. Rust, M. Bates, and X. W. Zhuang, "Sub-diffraction-limit imaging by stochastic optical reconstruction microscopy (STORM)," Nat. Methods **3**(10), 793–795 (2006).
11. M. Sackrow, C. Stanciu, M. A. Lieb, and A. J. Meixner, "Imaging nanometre-sized hot spots on smooth au films with high-resolution tip-enhanced luminescence and raman near-field optical microscopy," Chem. Phys. Chem. **9**(2), 316–320 (2008).
12. C. Stanciu, M. Sackrow, and A. J. Meixner, "High NA particle- and tip-enhanced nanoscale raman spectroscopy with a parabolic-mirror microscope," J. Microsc. **229**(2), 247–253 (2008).
13. R. Zondervan, F. Kulzer, M. A. Kol'chenko, and M. Orrit, "Photobleaching of rhodamine 6G in poly(vinyl alcohol) at the ensemble and single-molecule levels," J. Phys. Chem. A **108**(10), 1657–1665 (2004).
14. W. E. Moerner and M. Orrit, "Illuminating single molecules in condensed matter," Science **283**(5408), 1670–1676 (1999).
15. R. Kaufmann, C. Hagen, and K. Grunewald, "Fluorescence cryo-microscopy: current challenges and prospects," Curr. Opin. Chem. Biol. **20**, 86–91 (2014).
16. M. Hussels, A. Konrad, and M. Brecht, "Confocal sample-scanning microscope for single-molecule spectroscopy and microscopy with fast sample exchange at cryogenic temperatures," Rev. Sci. Instrum. **83**(12), 123706 (2012).
17. R. Kaufmann, P. Schellenberger, E. Seiradake, I. M. Dobbie, E. Y. Jones, I. Davis, C. Hagen, and K. Grunewald, "Super-resolution microscopy using standard fluorescent proteins in intact cells under cryo-conditions," Nano Lett. **14**(7), 4171–4175 (2014).
18. S. Weisenburger, B. Jing, A. Renn, and V. Sandoghdar, "Cryogenic localization of single molecules with angstrom precision," Proc. SPIE **8815**, 88150D (2013).
19. S. Weisenburger, B. Jing, D. Hanni, L. Reymond, B. Schuler, A. Renn, and V. Sandoghdar, "Cryogenic colocalization microscopy for nanometer-distance measurements," Chem. Phys. Chem. **15**(4), 763–770 (2014).
20. Y. Shibata, W. Katoh, T. Chiba, K. Namie, N. Ohnishi, J. Minagawa, H. Nakanishi, T. Noguchi, and H. Fukumura, "Development of a novel cryogenic microscope with numerical aperture of 0.9 and its application to photosynthesis research," BBA-Bioenergetics **1837**(6), 880–887 (2014).
21. M. Yoshita, T. Sasaki, M. Baba, and H. Akiyama, "Application of solid immersion lens to high-spatial resolution photoluminescence imaging of GaAs quantum wells at low temperatures," Appl. Phys. Lett. **73**(5), 635–637 (1999).
22. M. Vollmer, H. Giessen, W. Stolz, W. W. Ruhle, L. Ghislain, and V. Elings, "Ultrafast nonlinear subwavelength solid immersion spectroscopy at t = 8 K," Appl. Phys. Lett. **74**(13), 1791–1793 (1999).
23. W. X. Li, S. C. Stein, I. Gregor, and J. Enderlein, "Ultra-stable and versatile widefield cryo-fluorescence microscope for single-molecule localization with sub-nanometer accuracy," Opt. Express **23**(3), 3770–3783 (2015).
24. C. L. Schwartz, V. I. Sarbash, F. I. Ataullakhanov, J. R. Mcintosh, and D. Nicastro, "Cryo-fluorescence microscopy facilitates correlations between light and cryo-electron microscopy and reduces the rate of photobleaching," J. Microsc. **227**(2), 98–109 (2007).
25. A. Rigort, E. Villa, F. J. B. Bauerlein, B. D. Engel, and J. M. Plitzko, "Integrative approaches for cellular cryo-electron tomography: Correlative imaging and focused ion beam micromachining," Methods Cell Biol. **111**, 259–281 (2012).
26. L. F. van Driel, J. A. Valentijn, K. M. Valentijn, R. I. Koning, and A. J. Koster, "Tools for correlative cryo-fluorescence microscopy and cryo-electron tomography applied to whole mitochondria in human endothelial cells," Eur. J. Cell Biol. **88**(11), 669–684 (2009).
27. A. Briegel, S. Y. Chen, A. J. Koster, J. M. Plitzko, C. L. Schwartz, and G. J. Jensen, "Correlated light and electron cryo-microscopy," Methods Enzymol. **481**, 317–341 (2010).
28. M. Schorb and J. A. G. Briggs, "Correlated cryo-fluorescence and cryo-electron microscopy with high spatial precision and improved sensitivity," Ultramicroscopy **143**, 24–32 (2014).
29. P. Anger, A. Feltz, T. Berghaus, and A. J. Meixner, "Near-field and confocal surface-enhanced resonance raman spectroscopy at cryogenic temperatures," J. Microsc. **209**, 162–166 (2003).
30. M. A. Le Gros, G. McDermott, M. Uchida, C. G. Knoechel, and C. A. Larabell, "High-aperture cryogenic light microscopy," J. Microsc. **235**(1), 1–8 (2009).
31. E. A. Smith, B. P. Cinquin, M. Do, G. McDermott, M. A. Le Gros, and C. A. Larabell, "Correlative cryogenic tomography of cells using light and soft x-rays," Ultramicroscopy **143**, 33–40 (2014).
32. T. L. Jennings, S. G. Becker-Catania, R. C. Triulzi, G. L. Tao, B. Scott, K. E. Sapsford, S. Spindel, E. Oh, V. Jain, J. B. Delehanty, D. E. Prasuhn, K. Boeneman, W. R. Algar, and I. L. Medintz, "Reactive semiconductor nanocrystals for chemoselective biolabeling and multiplexed analysis," ACS Nano **5**(7), 5579–5593 (2011).
33. W. W. Yu, L. H. Qu, W. Z. Guo, and X. G. Peng, "Experimental determination of the extinction coefficient of

#261789 Received 18 Apr 2016; revised 27 May 2016; accepted 27 May 2016; published 6 Jun 2016

CdTe, CdSe, and CdS nanocrystals," Chem. Mater. **15**(14), 2854–2860 (2003).
34. M. Hussels, M. Brecht, "Vorrichtung und Verfahren zum Transferieren eines Probenhalters von einer Transportvorrichtung zu einer Scanvorrichtung," Patent DE102012218377 B3, April 17 (2014).
35. K. Moutzouris, M. Papamichael, S. C. Betsis, I. Stavrakas, G. Hloupis, and D. Triantis, "Refractive, dispersive and thermo-optic properties of twelve organic solvents in the visible and near-infrared," Appl. Phys. B **116**(3), 617–622 (2014).
36. V. Hirschfeld and C. G. Hubner, "A sensitive and versatile laser scanning confocal optical microscope for single-molecule fluorescence at 77 K," Rev. Sci. Instrum. **81**(11), p. 113705, Nov. 2010.
37. F. Grazioso, B. R. Patton, and J. M. Smith, "A high stability beam-scanning confocal optical microscope for low temperature operation," Rev. Sci. Instrum. **81**(9), 093705 (2010).
38. A. Konrad, F. Wackenhut, M. Hussels, A. J. Meixner, and M. Brecht, "Temperature dependent luminescence and dephasing of gold nanorods," J. Phys. Chem. B **117**(41), 21476–21482 (2013).
39. J. Dubochet, "The physics of rapid cooling and its implications for cryoimmobilization of cells," Methods Cell Biol. **79**(79), 7–21 (2007).
40. C. van Rijnsoever, V. Oorschot, and J. Klumperman, "Correlative light-electron microscopy (CLEM) combining live-cell imaging and immunolabeling of ultrathin cryosections," Nat. Methods **5**(11), 973–980 (2008).

1. Introduction

Light microscopy is an often used technique especially for investigating biological samples and in combination with spectroscopy for getting a deeper understanding of chemical and physical processes with high spatial resolution. Confocal microscopy developed by Marvin Minsky in 1957 [1] was a remarkable step in optical microscopy that increased the imaging contrast for gaining spatial information on luminescent samples. The principle of confocal microscopy relies on focusing a laser beam to a diffraction limited spot and recording light emerging mainly from that volume. In this technique out-of-focus light will be suppressed and hence increases the image contrast and enables to record 3D images of different structures such as biological cells by implementing a pinhole in front of the detector [2]. Therefore, a high numerical aperture (NA) microscope objective (MO) with corrected aberrations is required for high quality imaging with a high axial and lateral resolution. The NA describes the acceptance cone of an objective (see Eq. (1)):

$$NA = n\sin(\alpha), \tag{1}$$

where n is the refractive index of the medium between the lens and the sample and α is half the opening angle of a focusing element. Hence, for extended samples the NA in air ($n_{air} = 1$) can never be larger than unity, which could be achieved e.g. by a parabolic mirror [3]. In order to increase the NA and thus the resolution of a microscope beyond unity an additional immersion fluid, such as water or immersion oil is used. The principle of immersion requires to fill the volume between the MO and sample by a transparent medium with a high refractive index. Using immersion liquids also increases the collection efficiency of the MO by reducing refraction and reflection at the interfaces between MO and sample. Nevertheless, the lateral resolution of light microscopes is typically restricted to the diffraction limit given by [4]:

$$d = \frac{\lambda}{2NA}, \tag{2}$$

where λ is the wavelength of light in vacuum and d is the minimal distance at which to identical point like sources can be resolved. Since several years, the diffraction limit hampering high resolution microscopy of nanoscopic particles or structures (size below 200 nm) was overcome by various super-resolution techniques at ambient conditions [5–12]. However, many chromophores or auto-fluorescent proteins are difficult to observe at room temperature especially at the single molecule level due to their low signal intensities, various quenching effects and fast photo-bleaching [13]. Further problems related to biological samples are drifts and degradation during measurements. One common solution for all these problems can be achieved by

#261789 Received 18 Apr 2016; revised 27 May 2016; accepted 27 May 2016; published 6 Jun 2016

reducing the temperature. This reduces photobleaching and enhances the fluorescence signal up to two orders of magnitude. Low temperature experiments of biological samples allow us to record fluorescence images without additional labeling [14]. Furthermore, effects of many biological samples like drifting and degradation are also eliminated. However, confocal cryogenic microscopy is challenging due to technical and mechanical requirements of the low temperatures environment. Beam scanning and widefield imaging as common techniques at cryogenic temperatures cannot reach a high resolution and image quality comparable to ambient conditions because the MOs for low temperatures are insufficiently corrected for aberrations. The reason for that is, that most high-performance MOs are corrected for room temperatures and lose their high imaging properties under cryogenic conditions and getting easily damaged by thermal stress [15]. Using confocal sample scanning instead of beam-scanning the lower off-axis performance of the MO at low temperatures is not important for the image quality [16]. A further hurdle - if one aims to implement high-resolution techniques at low temperatures - is the low longterm stability of the whole setup. These instabilities are caused by temperature gradients at the interface between the room and the low temperatures segments of the setup [15]. Nevertheless, several approaches to increase the resolution of microscopes at cryogenic temperatures could be achieved. Kaufmann *et al.* [17] utilize the effect of photoswitching [18, 19] of fluorescent marker proteins by using a 0.75 NA MO for super-resolution fluorescence cryogenic-microscopy. Shibata *et al.* developed a microscope with NA of 0.9, where the MO is mounted inside of the cryogenic vacuum space [20]. One method exceeding an NA of unity, was achieved by using solid immersion lenses [21] exhibiting an NA of 1.23 [22] with the disadvantage of a very small field of view. A versatile widefield cryo-fluorescence microscope for single molecule localization with good thermal and mechanical stability was recently developed by Li *et al.* [23], featuring however an NA of only 0.7. A further often used technique combines low temperatures fluorescence microscopy with other imaging techniques like electron microscopy. One example bases on the application of long working distance MOs with NA of 0.7 [24] or 0.75 [25, 26] and is able to combine cryogenic fluorescence microscopy with cryo-electron microscopy [27]. Another setup developed by Schorb *et al.* applies a short working distance MO with an NA of 0.95 in combination with electron microscopy [28]. However, until today none of these techniques were able to provide a resolution and image quality compared to conventional microscopes at ambient conditions. Only with a parabolic mirror as focusing element a diffraction limited resolution and an NA close to unity was demonstrated at 8.5 K along with a large scanning range [29]. The decisive factor under cryogenic conditions is that the simple application of immersion fluids to provide an NA higher than unity is exceedingly problematic due to their high freezing temperatures. One promising brightfield imaging approach to increase the resolution under cryogenic temperatures by immersing the microscope was reported by Le Gros *et al.* [30, 31]. They use liquid propane or iso-pentane as immersion fluids and an MO placed outside the sample area, cooled with a copper cooling strip by liquid nitrogen. Summarizing, all these techniques may reach a resolution comparable to microscopes at ambient conditions but at the cost of scan range, image quality or mechanical stability.

In this study, we present a microscope setup, which allows us to immerse an MO ($NA = 1.25$) together with the sample both positioned inside the sample chamber of a cryostat. Thus, we are able to record confocal luminescence images with an imaging resolution comparable to ambient conditions and scan ranges only limited by the travel range of the piezo steppers (limited to 15×15 mm). Additionally, combining our large range scanning stage [16] with a sample transfer system allows us to load frozen or vitrified samples into the cold cryostat and remove them after the measurements without heating the samples to ensure a reproducible cryogenic cycle [34]. We demonstrate the capability of our approach by confocally imaged quantum dots (QD) at 160 K with 1-propanol immersed MO and could appoint a resolution enhancement of

#261789 Received 18 Apr 2016; revised 27 May 2016; accepted 27 May 2016; published 6 Jun 2016

1.3 in comparison to our $NA = 0.85$ air objective.

2. Experimental setup

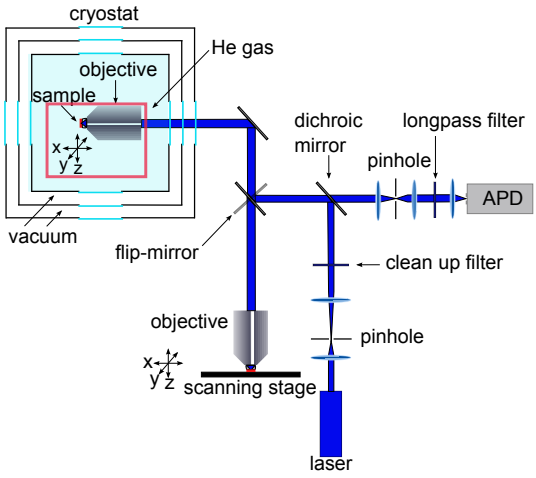

Fig. 1. Sketch of the low and room temperature setup for confocal imaging.

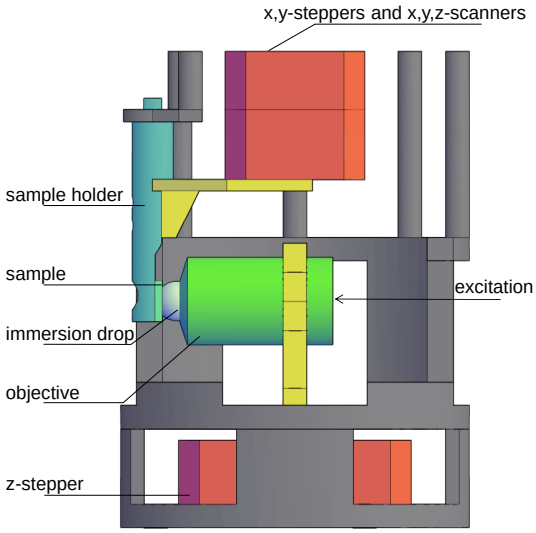

Fig. 2. Sketch of the focusing system (red quadrangle in Fig. 1) for low temperature microscopy adapted from [16]. With a special sample transfer system, consisting of x, y, z, steppers (red), to transfer frozen (also vitrified) samples into the precooled cryostat.

According to the manufacturer (ebioscience), the QDs have the following properties: Amine-Functionalized eFluor(R) 650NC nanocrystal consisting of CdSe/ZnS with a diameter of about 8.7 nm [32]. As a result, the QDs can be regarded as point light sources enabling us to estimate the resolution by means of the FWHM of the PSFs. The QDs exhibit a relativly high absorption

#261789 Received 18 Apr 2016; revised 27 May 2016; accepted 27 May 2016; published 6 Jun 2016

cross section, a large luminescence quantum yield, a molar extinction coefficient of 1.11E6 and an emission maximum around 650 nm without any sidebands and a high photostability [33]. A droplet (1 μl) of QDs solution diluted in H_2O/glycerol with concentration 1 $pmol/l$ to guaranty single particle microscopy was deposited between two 4 $\times$ 4 mm^2 (thickness 200 μm) glass coverslips cleaned with chromosulfuric acid. For the room temperature experiments, we used two 22 $\times$ 22 mm^2 coverslips and immersion oil (Zeiss Immersol 518 F). For the low temperature experiments, we used 1-propanol as immersion fluid due to its low melting point (147 K) and good transparency. The measurements were performed with a home-built confocal microscope consisting of a room and low temperature branch shown in Fig. 1. An enlarged section of the sample transfer system (red quadrangle in Fig. 1) and the low temperature sample head are shown in Fig. 2. Scanning the sample with nanometer precision was achieved at ambient condition by a feed-back controlled three axis scanning table (Physik Instrumente P-517.3CL, 100 $\times$ 100 $\times$ 20 μm) and at low temperatures by a multiaxis scanning stage (attocube steppers twice ANPx320 for x- and y-, ANPz101eXT for z-axis, scanners ANSxy100lr for x- and z-, ANSz100lr for y-axis) in a Helium-cryostat (Janis, SVT-200). The voltage dependent expansion of the scanners and their linearity were calibrated for low temperature (160 K) by scanning a copper grid (2000 lines/inch). The temperature dependent expansion deviation of the piezo scanners could be determined by the calibration measurements allowing us to calculate the spatial expansion of the scanners very accuratly. For the immersion measurements at room and low temperature we used an MO with high NA (Microthek, 100 $\times$, $NA = 1.25$) and as a reference at low temperature an air MO (Microthek, 60 $\times$, $NA = 0.85$) without immersion liquid. The temperature of 160 K in He atmosphere controlled by a cernox sensor (CX-1030-SD-HT 0.3L) is reached by cooling the outer temperature shield with liquid nitrogen. Temperature variations during the measurements can be minimized by an active temperature control sensor close to the sample [16]. The reliability of the microscope and the temperature control was demonstrated in a recent study [38]. A 488 nm *cw* laser diode (OBIS 488-20 LS) with a linear polarized Gaussian beam profile was used for exciting the QD. Their luminescence was collected by the very same MO passed a dichroic mirror, a 30 μm pinhole and a longpass filter (AHF F76-490) and was finally detected by an avalanche photodiode (APD, Laser Components, COUNT-100C). More details, of the setup were recently described by Hussels *et al.* [16].

3. Results

The immersion of the sample was achieved by applying a droplet of immersion liquid on the sample coverslip in three steps (Fig. 3). First we precool our sample holder with the mounted sample between two coverslips in a liquid nitrogen bath (Figs. 3(a) and 3(b)). After that a few droplets of 1-propanol were frozen directly on the coverslips (Figs. 3(c) and 3(d)).

A specially designed sample transfer mechanism allows us to insert the frozen sample into the precooled (140 K) cryostat without melting the immersion liquid [16]. Inside the cryostat the sample holder is translated towards the MO to achieve contact between the frozen immersion droplet and the MO. Then the sample chamber was heated slowly above the melting point (147 K) of 1-propanol to 160 K. Finally, we reduced the distance between sample and MO in order to bring the sample in the focus of the MO as shown in Fig. 2. Figure 4 shows confocal scanning images of luminescent QDs both at a temperature of 160 K with (right) and without immersion (left) excited with a 488 nm diode laser. The image on the left side was recorded with a commonly used air MO ($NA = 0.85$). On the right side, a segment of an image of the same QD sample recorded with a high numerical MO ($NA = 1.25$) immersed with 1-propanol is shown. Both images show symmetrical spots representing single QDs. However, the spot diameters become clearly smaller with higher theoretical NA (with immersion). Thus, no distortions, drifts or other instabilities even with the immersed MO for the respective temperature

#261789 Received 18 Apr 2016; revised 27 May 2016; accepted 27 May 2016; published 6 Jun 2016

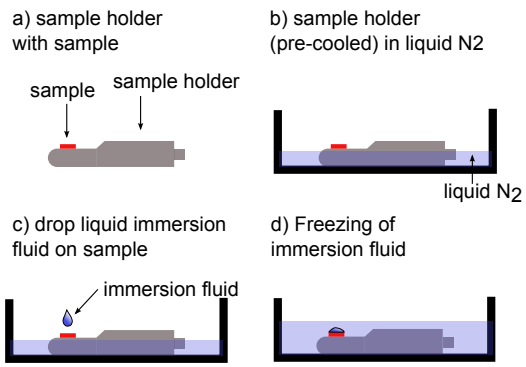

Fig. 3. Immersion procedure. a) Sample placed on sample holder b) precooled (liquid nitrogen) sample holder with sample c) applying of 1-propanol droplets directly on the glass coverslips d) freezing of 1-propanol.

disturb the measurements. However, the absolute intensities in Fig. 4 are not comparable due to different experimental conditions such as objective and sample changes. Furthermore not all QDs visible in the images are located in the focal plane causing individual excitation and luminescence yields.

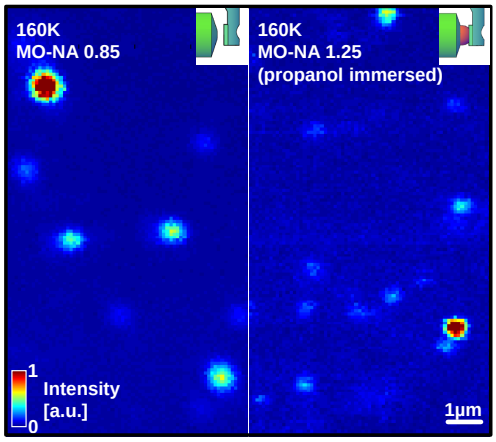

Fig. 4. Left: QD images recorded at 160 K with an air MO ($NA = 0.85$). Right: QD images recorded at 160 K with an immersion MO ($NA = 1.25$) with 1-propanol as immersion liquid.

To quantify the resolution of the respective MO reached by our experiments, we determine the point spread function (PSF) by scanning single QD in nanometer steps through the excitation focus. The excitation focus was generated by the linearly polarized ($\lambda = 488$ nm) beam with a diameter of 6 mm, filling the back aperture of the MO and can approximated by an Airy pattern with a nominal radius between the intensity maximum and the first intensity minimum of $r = 0,61 \cdot \frac{\lambda}{NA}$. As a reference measurement and to confirm the optical properties of the $NA = 1.25$ MO, we recorded several confocal images at 300 K immersed with standard immersion oil. Analyzing the line sections for these three conditions (160 K with 1-propanol immersion, 160 K without immersion and 300 K with oil immersion) allow us to determine the

#261789 Received 18 Apr 2016; revised 27 May 2016; accepted 27 May 2016; published 6 Jun 2016

full width of half maximum (FWHM) of the PSF for each single spot as a measure for the resolution. In Fig. 5 three spots are shown exemplarily for each condition, representing a single QD (Figs. 5(A1)–5(C1)) together with the line sections (Figs. 5(A2)–5(C2)) indicated by a white line in Figs. 5(A1)–5(C1). Figure 5(A1) shows the spatially resolved luminescence of a single QD at 160 K recorded with an air MO. The corresponding line section (Fig. 5(A2)) showing the luminescence intensity as function of the x-axis scanner position in μm (blue line) was fitted by a Gaussian (red line) in order to determine the FWHM of the lateral PSF. The usage of a Gaussian to reproduce the PSF is a well-founded approximation due to our linear Gaussian excitation beam and the small size of the emitter working as a point light source [8]. Figure 5(B1) shows one spot out of many from an image recorded with the 1-propanol immersed $NA = 1.25$ MO of the same QD sample. Figures 5(C1) and 5(C2) show images and corresponding line sections recorded with the same MO at 300 K immersed with standard immersion fluid (Zeiss Immersol^{T}M 518 F). Obviously these three line sections are all symmetric and scale inversely with the theoretical effective NA as expected. Figures 5(A3)-(C3) show the distribution of the FWHM for each condition.

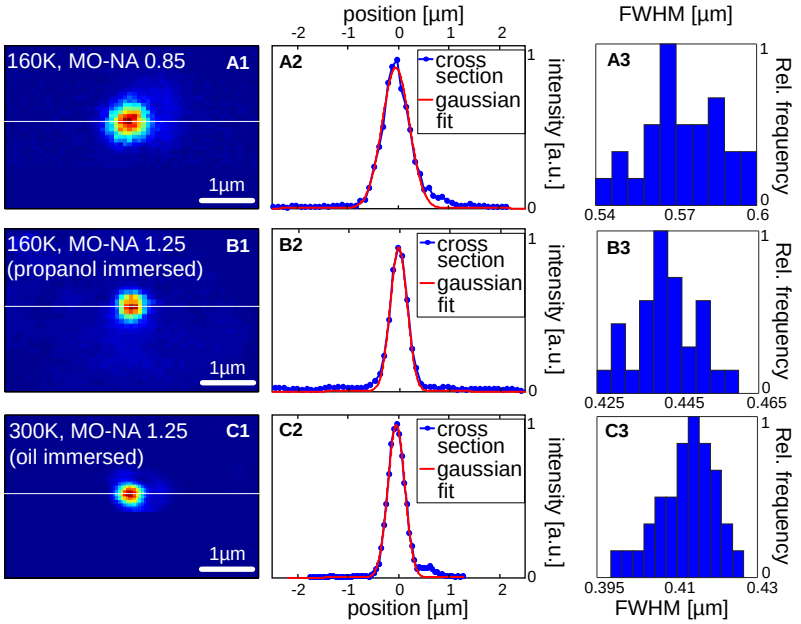

Fig. 5. Left: Three confocal luminescence images showing each a single QD recorded for different conditions. A1) enlarged section of a QD at 160 K recorded with an air MO with an $NA = 0.85$. A2) line section (blue line) indicated by the white line in Fig. A1 with Gaussian fit (red line, $FWHM = 0.574$ μm) to determine the PSF. A3) distribution of the FWHM measured with an air MO. B1) confocal image of a QD at 160 K with 1-propanol immersed MO ($NA = 1.25$). B2) line section (blue line) indicated by the white line in Fig. B1 with Gaussian fit (red line, $FWHM = 0.442$ μm). B3) distribution of the FWHM measured with an immersion MO immersed with 1-propanol. C1) confocal image of a QD at 300 K with the same MO ($NA = 1.25$) oil immersed. C2) line section (blue line) indicated by the white line in Fig. C1 with Gaussian fit (red line, $FWHM = 0.415$ μm). C3) distribution of the FWHM measured with an immersion MO immersed with immersion oil.

Table 1 summarizes the results for the three different measuring conditions. The column in bold shows the results of our 1-propanol immersed measurements with a resolution enhance-

#261789 Received 18 Apr 2016; revised 27 May 2016; accepted 27 May 2016; published 6 Jun 2016

ment of 1.3 in comparison to our air objective and a comparable resolution to ambient conditions (right column).

Table 1. Comparison of our experimental results with an air objective, an oil immersed objective and the same objective immersed with 1-propanol.

	air objective	**immersion objective**	immersion objective
Temperatur [K]	160	**160**	300
Immersion Liquid	–	**1-propanol**	immersion oil
Refractive Index [at 300 K]	1.0	**1.3851 [35]**	1.518
FWHM [nm]	574	**442**	415
resolution enhancement	–	**1.3**	1.38

4. Discussion

The scan images recorded with the 1-propanol immersed MO show obviously comparable quality, scan range and resolution with respect to experiments at ambient conditions. Hence, we can claim that the lateral resolution of the immersed MO under cryogenic conditions is enhanced by a factor of 1.3 with respect to our standard air objective with $NA = 0.85$. Furthermore, all recorded images show no distortions, drifts or thermally induced variations of the sample position or the scanner translation. This is a result of the microscope design whereby the optical elements, the sample and the scanning stage are in a controllable thermally stable equilibrium.

The resolution enhancement arises from the increased refractive index of the 1-propanol with respect to helium as the medium between MO and sample coverslip. The NA depends linearly on the refractive index contributes linearly to the resolution of images acquired by fluorescence microscopy. The mismatch of the refractive indices between glass and 1-propanol are leading only to a reduced effective NA with respect to standard oil. We used 1-propanol as immersion fluid due to its melting point and its hydrophobic properties (high stability on glass substrates). Due to the lower refractive index of 1-propanol ($n_{532\ nm,300\ K} = 1.385$ [35] as compared to immersion oil ($n_{546,1\ nm,298\ K} = 1.518$) and the large number of optical elements (cryo windows) we estimated an enhancement factor around 1.3 compared to 1.38 with oil. To our knowledge we found no appropriate refractive index for 160 K. Hence, we make the following assumption using the TOC-value of 1-propanol of -4×10^{-4} resulting in a refractive index of 1.46 for 160 K [35].

For measuring our sample under cryogenic conditions, which is previously immersed outside the croystat a sample transfer system is indispensable. Our patented sample transfer system in combination with a sample scanning stage, instead of beam-scanning [36, 37], allows us to quickly insert (and remove) samples with attached frozen immersion droplets, into the precooled cryostat. Additionally, the optical properties of the whole setup will be increased by using sample scanning. Typical microscopes with cryo stages commonly use air MOs with a long working distance limiting the NA < 1 [24–26]. However, cryogenic systems with a high long term stability and NA close to unity usually do not feature the possibility of a transfer system [20]. Our method combines short working distance immersion MOs with an NA of 1.25 and a sample scanning stage allowing us to keep the whole microscope at a defined temperature. As a result, we have a mechanically stable system without temperature gradients resulting in a high imaging quality and stability which is a prerequisite for high resolution techniques such as STORM. In order to image vitrified cells (below 135 K [39]) however the immersion fluid has to be varied to reach a temperature below 135 K.

The improved spatial resolution of the developed method will be further applicable to correlative microscopy [27], which is a recently emerging technique combining cryo-electron to-

#261789 Received 18 Apr 2016; revised 27 May 2016; accepted 27 May 2016; published 6 Jun 2016

mography and fluorescence microscopy.

5. Conclusion

We demonstrated the resolution enhancement by applying an immersion fluid under cryogenic temperatures. This could be shown by determing the FWHM of confocally imaged QDs whereas an effective resolution enhancement of 1.3 compared to an air objective was achieved. Key to our experiment is the transfer mechanism which allows to insert a cooled sample with a frozen droplet of immersion liquid into the precooled cryostat and to bring it into contact with the objective lense. By our method of resolution enhancement at low temperature new opportunities can be realized e.g. the observation of biological systems, which can be imaged by their auto-fluorescence without additional labeling. The used sample transfer system together with our presented technique to immerse MOs at low temperature is therefore also of great relevance for correlative light and electron cryo microscopy (cryoCLEM) [27, 40]. With our long-term stable system without any temperature gradients super resolution methods like STED and STORM, which require a mechanical stability and high NA MO are also conceivable.

Acknowledgments

We gratefully acknowledge financial support by Baden-Wuerttemberg Stiftung and Deutsche Forschungsgemeinschaft. We thank the Kay Gruenewald group (division of structural biology, University of Oxford), especially Christoph Hagen and Rainer Kaufmann for helpful discussions.

#261789 Received 18 Apr 2016; revised 27 May 2016; accepted 27 May 2016; published 6 Jun 2016